Effect of Annealing on Structure and Optical Properties of GaTe Thin Films

M. M. El-Nahass[a] and M. H. Ali[b*]

[a] Physics Department, Faculty of Education, Ain Shams University, Roxy, Cairo 11757, Egypt.
[b]Physics Department, Faculty of Science, Ain Shams University, Abassia, Cairo11566, Egypt.*

GaTe thin films were deposited by thermal evaporation technique. The effect of annealing on the structure and optical properties was studied. X-ray diffraction of the as deposited films indicated that the films have a polycrystalline nature. Annealing at 473 K for 2 hours enhanced the crystallization and changed the preferential orientation from ($\bar{1}21$) plane for as deposited films to (110) plane for annealed films. Study of the optical band gap showed that; these films have direct band gap of 1.53 eV. Annealing increased the band gap to 1.62 eV. The effect of annealing on the optical parameters such as refractive index, extinction coefficient, dispersion energy parameters, and dielectric constants were investigated.

1. Introduction

The family of III–VI binary chalcogenide semiconductors has been extensively studied for decades because of their promising properties and technological applications. Among them, gallium monotelluride (GaTe) is of special interest which has a great potential use in Schottky device [1], as a window material for solar cells [2], radiation detectors [3-5], optoelectronic devices [6-8] as well as high performance high field effect transistor and phototransistor based on back-gated multilayer GaTe nanosheets [9].

GaTe is a layered semiconductor of less-studied III-VI semiconductors because of the complexity of the unit cell [10]. Several authors have studied the structure properties [11,12], electrical properties [13-15], and optical properties [10,16-22] of GaTe single crystals. There is discrepancy for the transition type as well as the value of the optical band gap. Yüksek et al. studied the nonlinear absorption properties of GaTe single crystal and reported an indirect band gap

of 1.6 eV [16]. Abed Rahman et al. studied the optical properties of GaTe single crystal at different temperatures [17]. They showed that the indirect forbidden energy gaps, at room temperature, were found to be 1.55 eV and 1.57 eV for three and two-dimensional models, respectively. Pellicer-Porres et al. studied the pressure dependence of the absorption coefficient of GaTe single crystals [18]. They reported that the absorption edge up to pressure of 6.1 GPa could be accounted for the superposition and interaction of a direct and an indirect band gap. The pressure shift of the direct gap was strongly nonlinear and exhibiting a minimum at pressure around 2.9 GPa. The band gap at atmospheric pressure was 1.68±0.004 eV. However, Zubiaga et al studied the emission spectra of GaTe single crystal using photoluminescence (PL), PL excitation and selective PL, the energy gap over 10-200 K was determined. The energy gap at 10 K was 1.796±0.001 eV [10]. The extrapolated band gap at 300 K was 1.641±0.001 eV. Cui et al. studied the deep-level transient spectroscopy (DLTS) and low temperature PL of GaTe single crystal and reported the band gap as 1.794 eV at 9 K [7]. Several authors reported GaTe single crystal to have direct band gap [19-22]. Cinai et al. reported that GaTe thin films grown on ITO substrate have direct band gap as 1.67 eV [1]. However, due to that discrepancy as well as there is no detailed information on the optical properties of GaTe in thin film form, as far as we know. Therefore, the aim of the present work is to investigate the optical properties as well as the effect of annealing on refractive index, extinction coefficient, dispersion energy parameters, and dielectric constants of GaTe thin films, which are essential to the understanding of the material and consequently their applications.

2. Experimental

2.1. Thin film deposition and characterization

Thin films of different thicknesses of GaTe (99.999 % Sigma, Aldrich) were thermally evaporated onto optically flat well-cleaned glass and quartz substrates from molybdenum boat using a high vacuum evaporation unit (Edward, E 306A). The vacuum pressure was maintained at about 1.3×10^{-4} Pa. The substrates fixed onto a rotatable holder to obtain homogenous films. The film thickness was monitored using a quartz thickness monitor (Edwards, FTM4) and finally checked by a multiple beam Fizeau method [23]. Samples with different thicknesses (33.6 nm-137 nm) were deposited under the same evaporation conditions.

The chemical composition of the deposited films was checked by analyzing the energy dispersion X-ray (EDX) spectroscopy data obtained using a scanning electron microscope (JEOL 5400). The experimental error in the

composition change was within the range of ± 2%, indicated that the films were nearly as expected composition. Thin films were annealed at 473 K for 2 hours in a vacuum of ~ 10^{-4} Pa and the temperature was monitored with Keithly multimeter (model 196) using Copper constantan thermocouple in contact with the sample. X-ray diffractometer (Phillips X′Pert) having CuK_{α} radiation operating at 40 kV and 30 mA was used to investigate the films.

The optical transmittance and reflectance of GaTe thin films of different thicknesses (33.6 to 137 nm) deposited on optically flat quartz substrates were measured, at room temperature, at normal incidence. Double beam spectrophotometer [JASCO Corp., V-570, and Rev.1.00.] was used in the wavelength range of 400 to 2500 nm. The obtained data from the spectrophotometer was transformed to their absolute values by eliminating the absorbance and reflectance of the quartz substrate. Therefore, the absolute values of *T* and *R* are given by [24]:

$$T = \left[\frac{I_{ft}}{I_q}\right](1 - R_q) \tag{1}$$

where I_{ft}, I_q are the intensities of light passing through the film-quartz system and reference quartz substrate, respectively and $R_q$is the reflectance of the quartz substrate, and

$$R = \left[\frac{I_{fr}}{I_m}\right] R_m \left(1 + [1 - R_q]^2\right) - T^2 R_q \tag{2}$$

where I_{fr}, I_m are the intensities of light reflected from the sample and the reference mirror, and R_m is the mirror reflectance. The experimental errors of the calculated values of *n* and *k* were found to be with accuracy better than ± 4%. Taken into account, the accuracy in measuring the film thickness, *T* and *R* were ±2% and ±1%, respectively. The experimental values of transmittance, reflectance (T_{exp} and R_{exp}) and film thickness (*d*) were used to calculate the refractive index, *n*, and extinction coefficient, *k*. In this work, a computer program is designed, as reported earlier [25-27], comprising a modified bi-variance search technique, based on minimizing $(\Delta R)^2$ and $(\Delta T)^2$, simultaneously, such that:

$$(\Delta T)^2 = \left|T_{(n,k)} - T_{exp}\right|^2 \tag{3}$$

$$(\Delta R)^2 = \left|R_{(n,k)} - R_{exp}\right|^2 \tag{4}$$

where $T_{(n,k)}$ and $R_{(n,k)}$ are the calculated values of *T* and *R* by using Murmann′s exact formulas [28,29].

3. Results and Discussions

3.1. Structure

Figure (1) shows the X-ray diffraction (XRD) patterns of as deposited GaTe thin films and that annealed at 473 K for 2 hours. The figure confirms the polycrystalline nature of the films. The indexing of XRD pattern shows that there is a reasonably good agreement between observed d-values and the published data [30]. XRD results suggest that GaTe thin films were monoclinic with a=17.404 Å, b=4.077 Å, c=10.456 Å and γ =104.77°. Monoclinic structure for GaTe single crystal was reported earlier [3]. These patterns show that annealing enhanced the crystallinity of the films and leads to the appearance of additional XRD diffraction peaks. Annealing changed the preferential orientation. The strongest diffraction peak of the films is changed from ($\bar{1}$21) plane for as deposited film to the (110) plane after annealing.

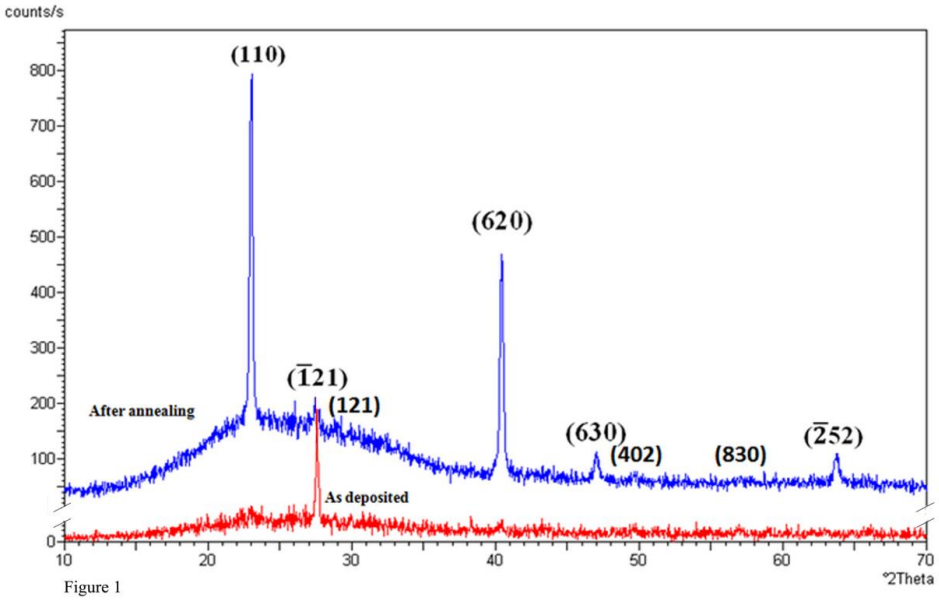

Fig. (1): X-ray diffraction pattern for as deposited GaTe thin films of thickness 51 nm and for film annealed at 473 k for 2 hours.

The crystallite size (*D*) of the as deposited and annealed GaTe thin films are calculated from XRD broadening of the planes (110), ($\bar{1}$21), (620), (630) and ($\bar{2}$52) using Scherrer's equation [31].

$$D = \frac{0.95\,\lambda}{w\cos\theta} \tag{5}$$

where λ is the X-ray wavelength, w is the peak width of the peak at half maximum intensity and θ is the diffraction angle. The calculated crystallite sizes are shown in Table 1. It is clear that the crystallite size of the plane ($\bar{1}21$) is reduced due to annealing. While, there are more intensive diffraction peaks were observed which have higher values of the crystallite size. These confirm that the crystallinity is improved upon annealing. It indicates that annealing of GaTe films leads to grain growth in the films. Zubiaga et al. was studied the PL emission of as grown and annealed GaTe single crystal, at 473 K for one hour, and reported that the crystallinity is improved with annealing [32].

Table (1): The crystallite size for different XRD planes for as deposited and annealed GaTe thin films

Film condition	(110) nm	($\bar{1}21$) nm	(620) nm	(630) nm	($\bar{2}52$) nm
As deposited films	-	35.22	-	-	-
Annealed films	47.54	28.78	42.55	38.10	65.82

3.2. Optical Properties

3.2.1. Spectral distribution of transmittance and reflectance

The spectral distribution of the transmittance T (λ) and reflectance R (λ) of as deposited and annealed GaTe thin films, of different thicknesses (33.6, 51.5, 80.5 and 137 nm) are shown in Fig. (2) a and b, respectively. It is clear from the figure that the films have low relatively transmission in both visible (λ = 400 to 800 nm) and near infrared region (NIR) (λ= 1800 to 2500 nm). Comparing the transmission, we noted that the transmission of annealed films is higher than that of as deposited films of the same thickness. This may be due to annealing effect, which enhanced the crystallinity of the films as indicated (Fig. 1- XRD).

3.2.2. Determination of optical constants

The absolute values of the transmittance, T and reflectance, R were used to calculate the refractive index, n and extinction coefficient, k. It was found that n and k were independent of the film thickness in the investigated wavelength range of 400-2500 nm. The refractive index, n (λ), for as deposited and annealed films are shown in Fig. (3). It is concluded that GaTe thin films had an anomalous dispersion in shorter wavelength range (λ<1000 nm) while,

normal dispersion in the wavelength range (λ>1100 nm). It is clear that, the refractive index increased by annealing. The refractive index increased to higher values at the same wavelength. Annealing caused a red shift for the dispersion curve of the refractive index.

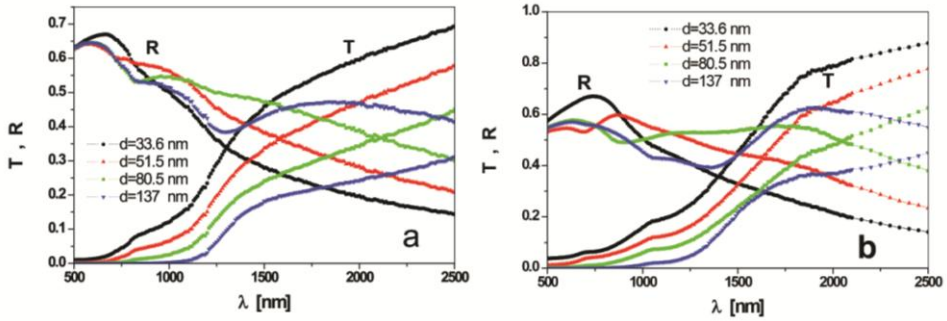

Fig. (2): The spectral distribution of transmittance (*T*) and reflectance (*R*) for GaTe thin films of different thicknesses (a) for as deposited films and (b) annealed films at 473 k for 2 hours.

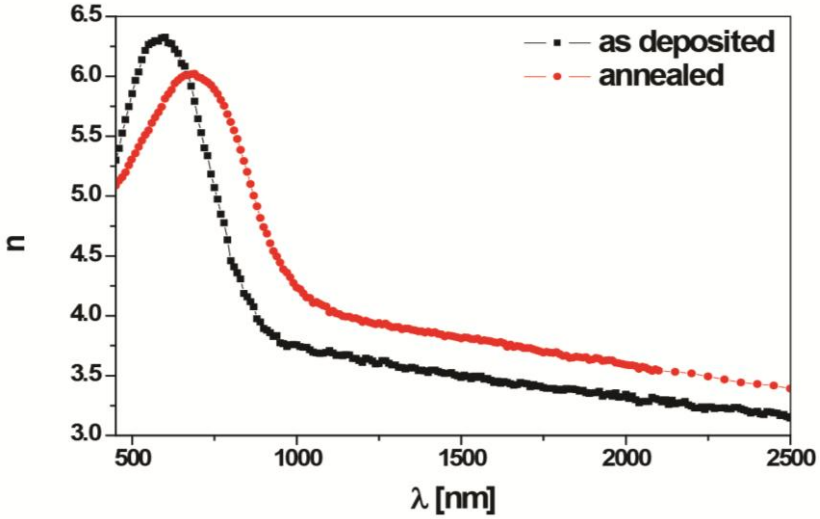

Fig. (3): The dependence of the refractive index (*n*) for as deposited and annealed GaTe thin films.

The spectral dependences of refractive index, *n* (hν) for as deposited and annealed GaTe thin films are shown in Fig. (4). One can observe that the refractive index, n exhibits a strong dispersion due to the onset of inter-band transitions and n reaches a maximum value of $n = 6.327$ at energy 2.067 eV and of $n = 6.022$ at energy 1.797 eV for as deposited and annealed films, respectively. The energy of the maximum value of *n* (2.067 eV) agreed with the single oscillator energy, as it will be explain in the next section.

3.2.3. Absorption and extinction coefficient

The absorption coefficient, α, could be obtained according to the relation

$$\alpha = 4\pi k/\lambda \quad (6)$$

where λ is the wavelength. The calculated absorption coefficient, α, versus photon energy ($h\nu$) is depicted in Fig. (5) for as deposited and annealed films. One can observe that α, increases with increasing photon energy. It was observed that the absorption edge shifted to higher energy with annealing. This may be due to the enhancement of the crystallinity.

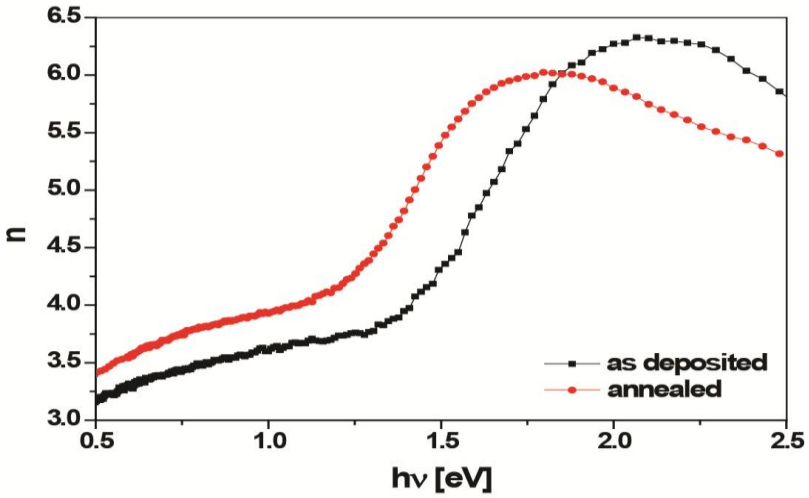

Fig. (4): The dependence of the refractive index (n) on the photon energy (hν) for as deposited and annealed GaTe thin films.

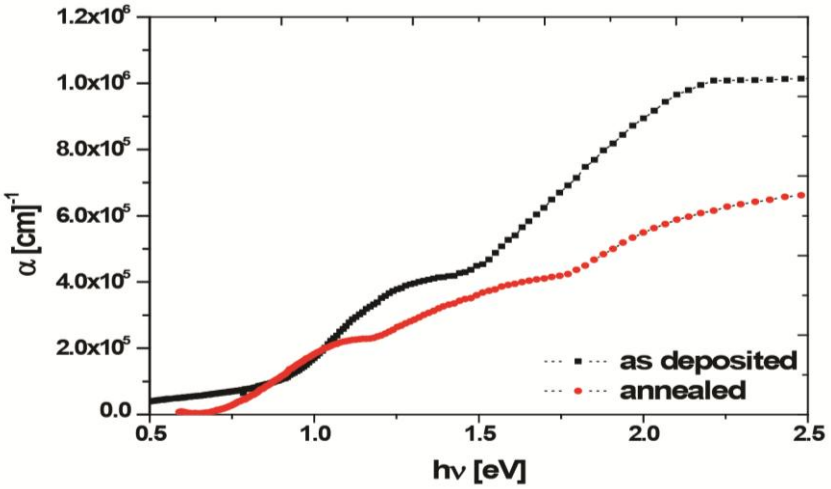

Fig. (5): The dependence of the absorption coefficient (α) versus the photon energy (hν) for as deposited and annealed GaTe thin films.

The absorption coefficient can be used to determine the optical band gap E_g^{opt} according to the relation:

$$\alpha h\nu = A\,(h\nu - E_g^{opt})^m \qquad (7)$$

where A is a constant, $h\nu$ is the photon energy and the exponent, m=1/2 for allowed direct and m=2 for allowed indirect transitions. The dependence of $(\alpha h\nu)^{1/m}$ and photon energy $(h\nu)$ were studied for different values of exponent m and the best fit was obtained for m=1/2. This indicates that GaTe thin films have allowed direct transition. The direct optical band gap was determined by extrapolating the linear portions of the curves $(\alpha h\nu)^2$ to zero absorption with the photon energy axis. Fig. (6) show the plot of $(\alpha h\nu)^2$ versus photon energy for as deposited and annealed GaTe thin films at 473 K for 2 hours. The figure confirms that GaTe thin film have direct band gap as reported earlier for GaTe single crystal [19-22] and confirms the direct band gap reported for GaTe thin film on ITO substrate as 1.67 eV [1].

It is clear from the figure that the direct band gap for as deposited GaTe films was 1.53 eV and it increased to 1.62 eV after annealing. The difference between the obtained results and the reported data may be due to the different preparation conditions.

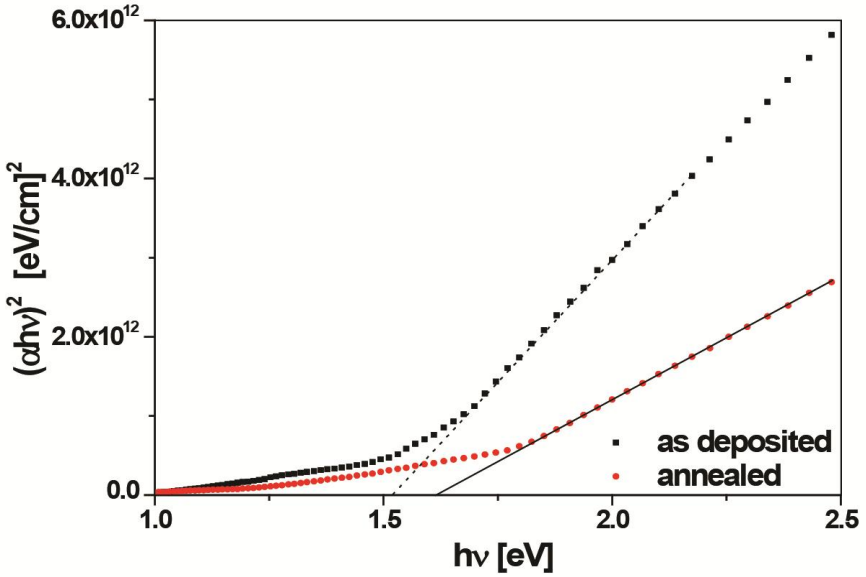

Fig. (6): The dependence of $(\alpha h\nu)^2$ versus the photon energy for as deposited and annealed films.

3.2.4. The Dispersion Energy Parameters

The dispersion refractive energy can be analyzed using the single oscillator model proposed by Wemple and Didomenico, (WDD) [33,34]:

$$n^2 - 1 = \frac{E_o E_d}{E_o^2 - (h\nu)^2} \quad (8)$$

where E_o and E_d are the energy of the effective dispersion oscillator and the dispersion energy, respectively. This is the measure of the average strength of interband optical transitions. Fig. (7) illustrates the graph of $(n^2-1)^{-1}$ versus $(h\nu)^2$ for as deposited and annealed GaTe thin films, which yields straight lines having the slope $(E_oE_d)^{-1}$ and the intercept is E_o/E_d. By extrapolating the linear part of WDD optical dispersion relationship towards the infrared spectral region (hν = 0), the refractive index n_∞, could be defined by the infinite wavelength dielectric constant ε_∞ and the deduced values are indicated in table 2. The obtained values of the parameters E_0 and E_d are given in Table 2.

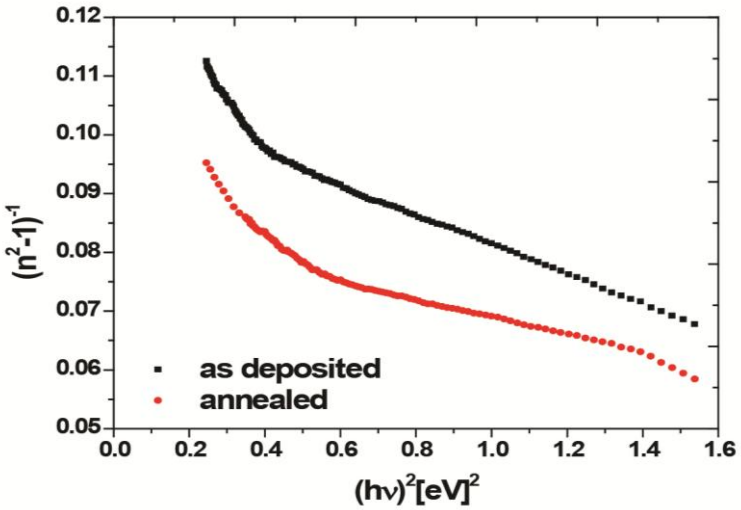

Fig. (7): The dependence of $(n^2-1)^{-1}$ on the square photon energy $(h\nu)^2$ for as deposited and annealed GaTe thin films.

Table (2): The parameters of E_o, E_d, ε_∞, ϵ_L and N/m^* for as deposited and annealed GaTe thin films.

Film condition	E_o (eV)	E_d (eV)	ε_∞	ϵ_L	N/m^* $Kg^{-1}m^{-3}$
As deposited films	2.059	19.345	10.393	13.352	6.909×10^{56}
Annealed films	2.388	28.528	12.947	16.778	1.203×10^{57}

3.2.5. Determination of the High Frequency Dielectric Constant

The high frequency lattice dielectric constant, ε_L, can be obtained using the relation [35]:

$$n^2 = \varepsilon_L - B\,\lambda^2 \tag{9}$$

where ε_L is the lattice dielectric constant, λ is the wavelength and B is given by $(\frac{e^2N}{4\pi^2c^2\varepsilon_o\ m^*})$ where e is the electronic charge, N is the free charge-carrier concentration, c is the speed of light, ε_o is the permittivity of free space, and m* is the electron effective mass.

Figure (8) shows the dependence of n^2 versus λ^2. Extrapolating the linear part to zero wavelengths gives the value of ε_L. The ratio N/m* can be calculated from the slopes of these lines. Table 2 shows the values of ε_L and N/m* for the investigated films. The difference between the values of ε_∞ and ε_L may be due to free carrier contribution. Table 2 shows an increase in the optical parameters after annealing. This may be due to enhancement of crystallinty and the change of the preferred orientation.

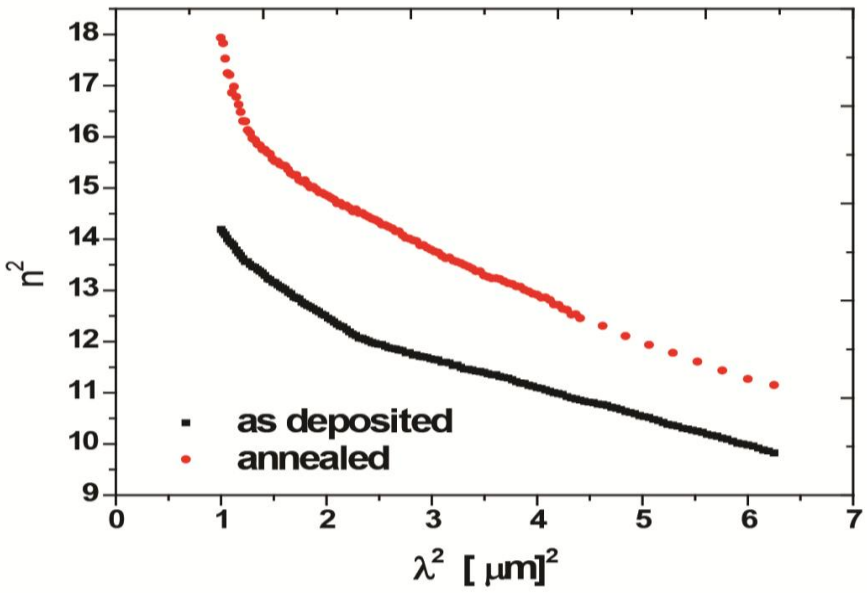

Fig. (8): The dependence of n^2 on the square wavelength (λ^2) for as deposited and annealed GaTe thin films.

3.2.6. Determination of the Complex Dielectric Constant near the Absorption Edge

The real and imaginary parts of the dielectric constant ϵ_1 and ϵ_2 of GaTe thin films (in the absorption region) were determined by the following relations [36]:

$$\varepsilon_1 = n^2 - k^2 = \varepsilon_L - \left(\frac{e^2 N}{4\pi^2 c^2 \varepsilon_0 m^*}\right) \lambda^2 \quad (10)$$

and

$$\varepsilon_2 = 2nk \quad (11)$$

Values of ε_1 and ε_2 can be calculated as it is directly related to the density of states within the forbidden gap [36]. Variation of ε_1 and ε_2 versus hν are shown in Fig. (9) for as deposited and annealed GaTe thin films. It is clear that ε_2 is higher than ε_1 at same energy. Fig. 9 (a, b) shows that with increasing photon energy, ε_1 and ε_2 increases. There is a maximum in ε_1 and corresponding a minimum of ε_2 at photon energies of 1.55 eV, and 1.78 eV, respectively. These may be an indication of the direct band gaps for as deposited and annealed films, respectively. The values of 1.55 eV and 1.78 eV were in agreement with that obtained from the absorption curves.

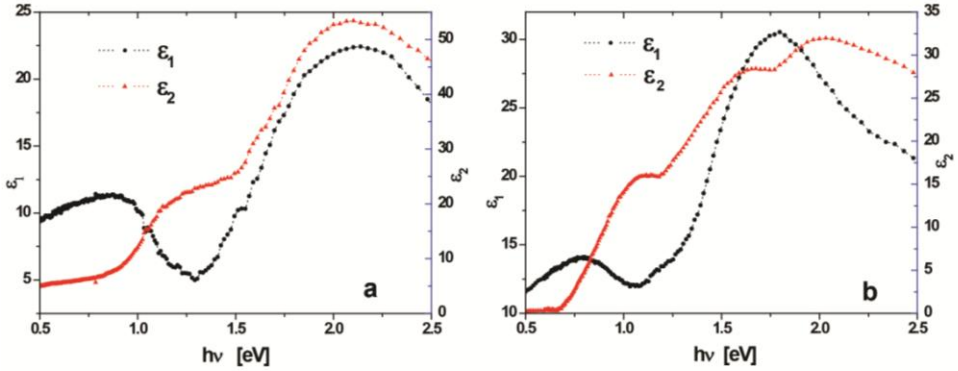

Fig. (9): Plots of ϵ_1 and ϵ_2 as a function of hν for (a) as deposited and (b) annealed GaTe thin films.

4. Conclusion

GaTe thin films were deposited by thermal evaporation technique in the thickness range 33.6 nm to 137 nm. X-ray diffraction analysis of as deposited and annealed films showed that these films were polycrystalline nature. Annealing enhanced the crystallinity of the films leading to grain growth and change the preferential orientation from ($\bar{1}$21) plane to (110) plane. The optical constants *n* and *k* of the GaTe thin films have been determined in the wavelength range 400-2500 nm using Murmann′s exact formulas. Both *n* and *k*

were practically independent of the film thickness in the investigated range. Analysis of the absorption coefficient indicated that the direct band gap for as deposited GaTe films were 1.53 eV and it increased to 1.62 eV after annealing. Analysis of the refractive index yields the ratio of the free charge carrier concentration to the effective mass ($N/m^*=6.909\times10^{56}$ $Kg^{-1}m^{-3}$), a high frequency dielectric constant ($\varepsilon_\infty=10.393$), the dispersion energy ($E_0=2.059$ eV) and the high frequency lattice dielectric constant ($\varepsilon_L=13.352$). The difference between ε_∞ and ε_L may be due to free carrier contributionn. Annealing increased these parameters due to enhancement of crystallinity and the change of the preferred orientation. The values of the real and imaginary parts of the dielectric constant increased with photon energy and confirmed the obtained value of the direct band gap.

References

1. K. Cinai, Z. Caldira, C. Coskun and S. Aydogan, *Thin Solid Films*, 550, **40** (2014).

2. K. C. Mandal, S. Das, R. Kirshna, P. G. Muzykov, S. Ma, and F. Zhao, *Mater. Res. Soc. Symp. Proc*., **1268**, 1268 (2010).

3. K. C. Mandal, R. M. Krishna, T.C. Hayes, P. G. Muzykov, S. Das, T. S. Sudarshan, and S. Ma, *IEEE Trans. on Nucl. Sci*., **58**, 1981 (2011).

4. A. J. Nelson, A. M. Conway, B.W. Sturm, E.M. Behymer, C. E. Reinhardt, R. J. Nikolic, S. A. Payne, G. Pabst, and K. C. Mandal, *J. Appl. Phys*., **106**, 023717 (2009).

5. A. J. Nelson, T.A. Laurence, A. M. Conway, E. M. Behymer, B. W. Strum. L. F. Voss, R. J. Nikolic, S. A. Payne, A. Metiri, G. Pabst, K. C. Mandal, A. Burger, *Mater. Lett*., **64**, 393 (2010).

6. K. C. Mandal, S. Kang, M. Choi, J. Chen, X. Zhang, J. M. Schleicher, C. A. Schmuttenmaer, and N. C. Fernelius, *IEEE J. Sel. Topics Quantum Electron*., **14**, 284 (2008).

7. Y. Cui, D. D. Caudel, P. Bhattacharya, A. Burger, K. C. Mandal, D. Johnstone, and S. A. Payne, *J. Appl. Phys*., **105**, 053709 (2009).

8. Z. Rak, S. D. Mahanti, K. C. Mandal, and N. C. Fernelius, *Phys. Rev*. B, **82**, 155203 (2010).

9. Z. Wang, K. Xu, Y. Li, X. Zhan, M. Safdar, Q. Wang, F. Wang and J. He, *Acs Nano*, **8**, 4859 (2014).

10. A. Zubiaga, J. A. García, F. Plazaola, V. Muñoz-Sanjosé and M. C. Martínez-Tomás, *J. Appl. Phys*., **92**, 7330 (2002).

11. O. A. Balitskii, B. Jaeckel, W. Jaegermann, *Phys. Lett*., A, **372**, 3303 (2008).

12. D. Olguin, A. Rubio-Ponce and A. Cantarero, *Eur. Phys. J*., B, **86**, 350 (2013).
13. G. Fisher, J. L. Brebner, *J. Phy. Chem of Solids*, **70**, 1363 (1962).
14. H. S. Güder, B. Abay, H. Efeoğlu, C. Coşkun, Ş. Aydoğan, Y. K. Yoğurtcu, Turkish, *J. of Phys*., **8**, 523 (2001).
15. H. Efeoğlu, T. Karacali, B. Abay and, Y. K. Yoğurtcu, Semicond. Sci. Technol., **19**, 523 (2004).
16. M. Yüksek, H. Ertap, A. Elmali, H. G. Yaglioglu, G. M. Mamedov, M. Kararabulut, M. K. Öztürk, *Optics & Laser Tech*., **44**, 2178 (2012).
17. M. Abdel Rahman and A. E. Belal, *J. Phys. and Chem. of Solids*, **61**, 925 (2000).
18. J. Pellicer-Porres, F.J. Manjón, A. Segura, V. Muñoz, C. Power and J. Gonzalez, *Phys. Rev*. B, **60**, 8871 (1999).
19. A. Yamamoto, A. Syouji, T. Goto, E.Kulatov, K.Ohno, Y. Kawazoe, K. Uchida, N. Miura, *Phys. Rev*., B, **64**, 035210 (2001).
20. J. F. Sánchez-Royo, A. Segura, and V. Muñoz, *Phys. Status Solidi* A, **151**, 257 (1995).
21. A. Gouskov, J. Camassel, and L. Gouskov, *Prog., Cryst., Growth Charact*., **5**, 323 (1982).
22. J. Camassel, P. Merle, and H. Mathieu, *Physica B & C*, **90,** 309 (1980).
23. S. Tolansky, Multiple Beam Interference Microscopy of Metals, Academic, London (1980).
24. M. M. El-Nahass, *J. of Mater. Sci*., **27**, 6597 (1992).
25. H. S. Soliman, N. El-Kadrry, O. Gamjoum, M. M. El-Nahass and H. B. Darwish, India, *J. Optics*, **17**, 46 (1972).
26. M. M. El-Nahass, H. S. Soliman, N. El-Kadry, A. Y. Morsy and S. Yagmour, *J. Mater. Sci. Lett*., **7**, 1050 (1988).
27. M. M. El-Nahass, F. Abd El-Salam, M. A. M. Seyam, *J. Mater Sci*., **41** 3573 (2006).
28. B. D. Mccombe, R. J. Wagner and J. S. Lannin, *Proc. XII Int. Conf. on the Physics of Semiconductors, Stuttgart*, 1176 (1974).
29. H. A. Macleod, "*Thin Films Optical*", Adam Hilger, Bristol, England, (1986).
30. Joint Comm. on Powder Diffraction Standard (JCPDS), Amer. Soc. for testing and Materials. (ASTM), **65**, 2208 (2002).
31. B.D. Cullity, S.R. Stocks, Elements of X-Ray Diffraction, Third ed., Prentic-Hall, (2001).
32. A. Zubiaga, J. García, F. Plazaola, V. Muñoz-Sanjosé, and C. Martínez-Tomás, Japan. *J. App. Phys*., **47**, 8719 (2008).
33. M. Didomenico, S. H. Wemple, *J. Appl. Phys.*, **40**, 720 (1969).
34. S. H. Wemple, M. Didomenico, *Phys. Rev*. B, **3**, 1338 (1971).

35. G. A. Kumar, J. Thomas, N. George, B. A. Kumar, P. R. Shnan, V. P. Npoori, C. P. G. Vallabhan, N. V. Unnikrishnan, *Phys. Chem. Glasses* **41**, 89 (2001).

36. M. M. Wakked, E. Kh. Shokr, S.H. Mohamed, *J. Non-Cryst. Solids*, **265**, 157 (2000).